Studies on the Light Polarization at the Longitudinal Polarimeter

S. Brauksiepe

April 1998

1 Light Polarization at the Interaction Point

At the longitudinal polarimeter the beam polarization P_Z is determined by the Compton asymmetry $A(E_\gamma)$, the analyzing power A_0 and the mean absolute polarization for left and right circularly polarized laser light ΔS_3:

$$P_Z = \frac{A(E_\gamma)}{\Delta S_3 \cdot A_0} \tag{1}$$

$$\Delta S_3 = \frac{1}{2} \cdot (S_{3,L} - S_{3,R}) \tag{2}$$

A precise measurement of ΔS_3 is important for a small systematic error of P_Z. The following sections deal with the experimental setup for the determination of ΔS_3.

1.1 The Problem

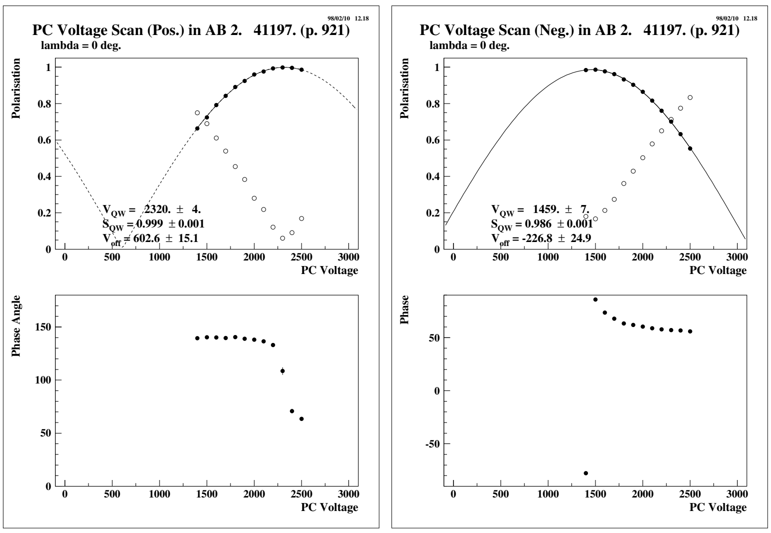

Figure 1: HV-Scans in the (probably broken) AB#2

The light polarization is normally measured during the operation of the polarimeter in an analyzer box (AB#2) which is installed in the tunnel behind the interaction point of the laser pulse and the electron beam. When we measured the circular polarization as a function of the applied high voltage at the Pockels cell, we found out that the optimum voltages for left and right circulary polarized light differ by about 850 Volts (see fig. 1). This means that our laser transport system and/or the AB#2 induce a phase shift which affects the measured polarization. During the data taking we tuned the high voltage in such a way that we observed highest circular polarization in the analyzer box which is installed in the laser hut (AB#1). The motivation for the following tests was to determine the error on the light polarization at the IP for the 1997 running period.

1.2 The Optical Setup

The main idea behind the measurements is to determine the variation of the maximum circular light polarization at the IP as a function of the original polarization produced in the laser hut.

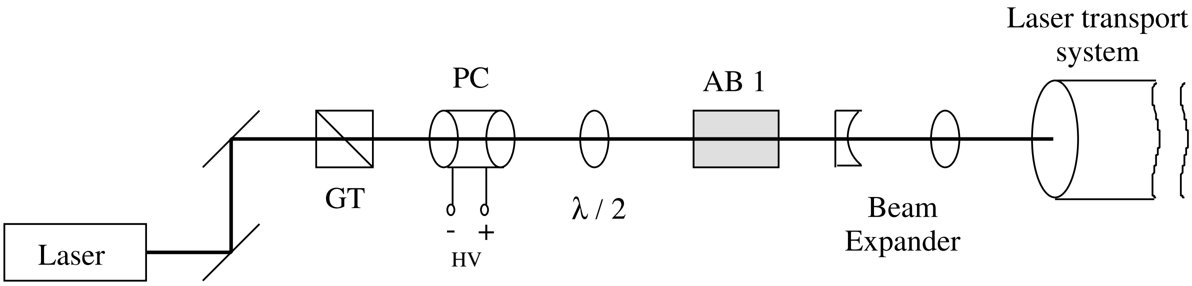

Figure 2: The optical setup

The first optical element behind the dog leg mirrors is a Glan-Thompson prism (GT) which ensures that the laser light is completely linear polarized. A Pockels cell (PC) converts the linear laser light into elliptically polarized light, depending on the applied high voltage. A half-wave plate rotates the orientation of the ellipse by an angle $\Delta\alpha$ which is twice the angle $\alpha_{\lambda/2}$, where $\alpha_{\lambda/2}$ denotes the angle between one principal axis of the ellipse and the (extra-)ordinary axis of the half-wave plate:

$$\Delta\alpha = 2 \cdot \alpha_{\lambda/2} \tag{3}$$

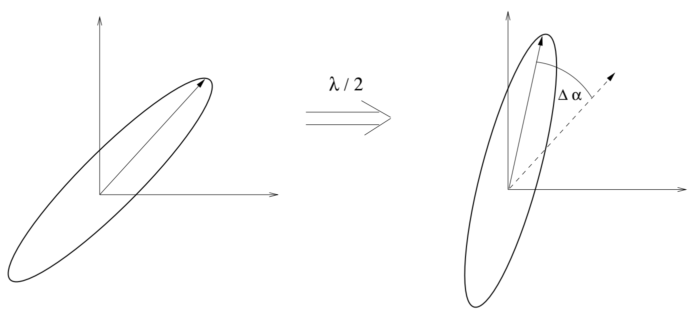

Figure 3: Rotation of elliptically polarized light

The polarization was measured with AB#1 moved to three points in the laser transport system (see fig. 4):

1. In the laser hut, behind the half-wave plate

2. Before the mirrors M5/6

3. Behind the Hera exit window (with AB#2 removed)

At each of these points so called "HV Scans" were performed in order to determine the variation of the maximum light polarization at a certain point as a function of the orientation of the ellipse in the laser hut. Unfortunately we didn't have enough time to perform these scans always over large angle ranges (which took ~15 hours), but one can clearly see the effects.

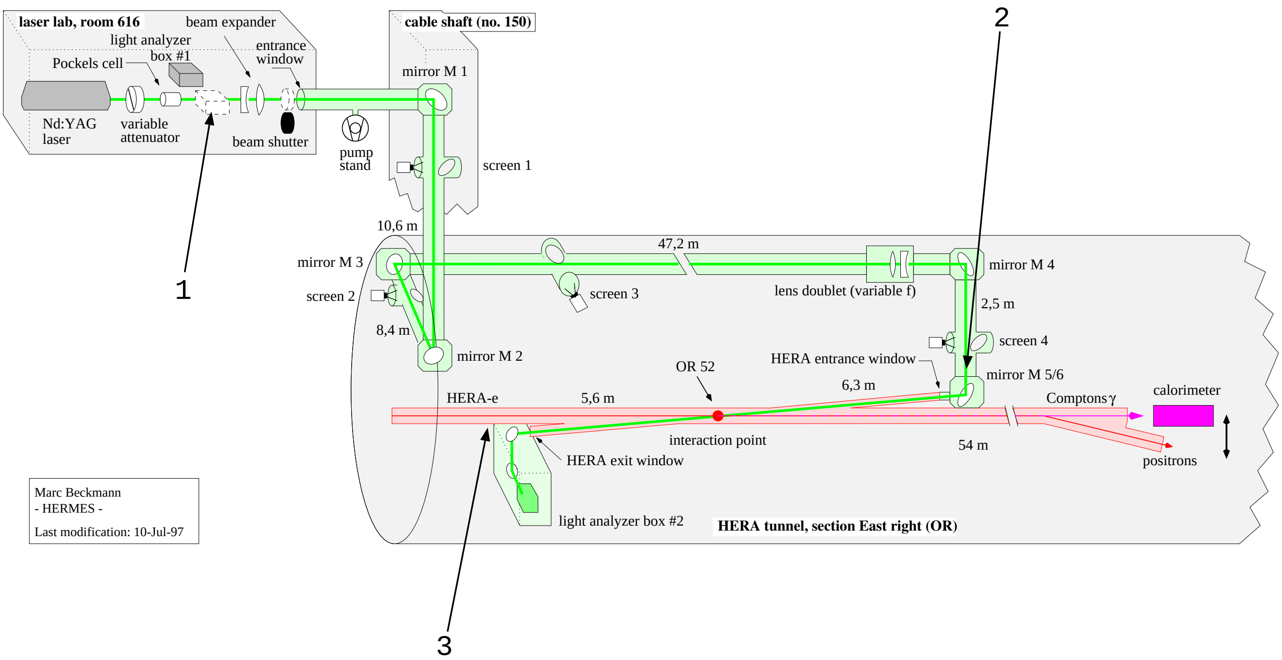

Figure 4: Layout of the laser transport system

1.3 Results

Figure 6 shows a full scan of the maximum light polarization in the laser hut. As one expects, the curve behaves (almost) like a $\sin(4\alpha)$ function. The reason why we do not observe a pure sine curve is due to the fact, that the phase shift of the half-wave plate is not exactly $\lambda/2$, which introduces a $\sin(2\alpha)$ component.
By comparing fig. 6 and fig. 8, we can see that all optical components including the hera entrance window cause a phase shift of $\sim 40°$. The hera exit window makes a small effect of $\sim 2°$. We were able to measure small linear components ($\leq 10\%$) of the light polarization behind the Hera exit window, at voltages which differ less than 300 Volts. This lead to the conclusion that the analyzer box #2 is not measuring the polarization in a proper way.

Figure 8 shows the polarization scan without the Hera exit window. Hence this measurement gives the polarization at the interaction point. The effect of the window on the measured polarization is smaller than 2% in the linear component.
Figure 5 shows the mean linear polarisation ΔS_1 as a function of the orientation angle:

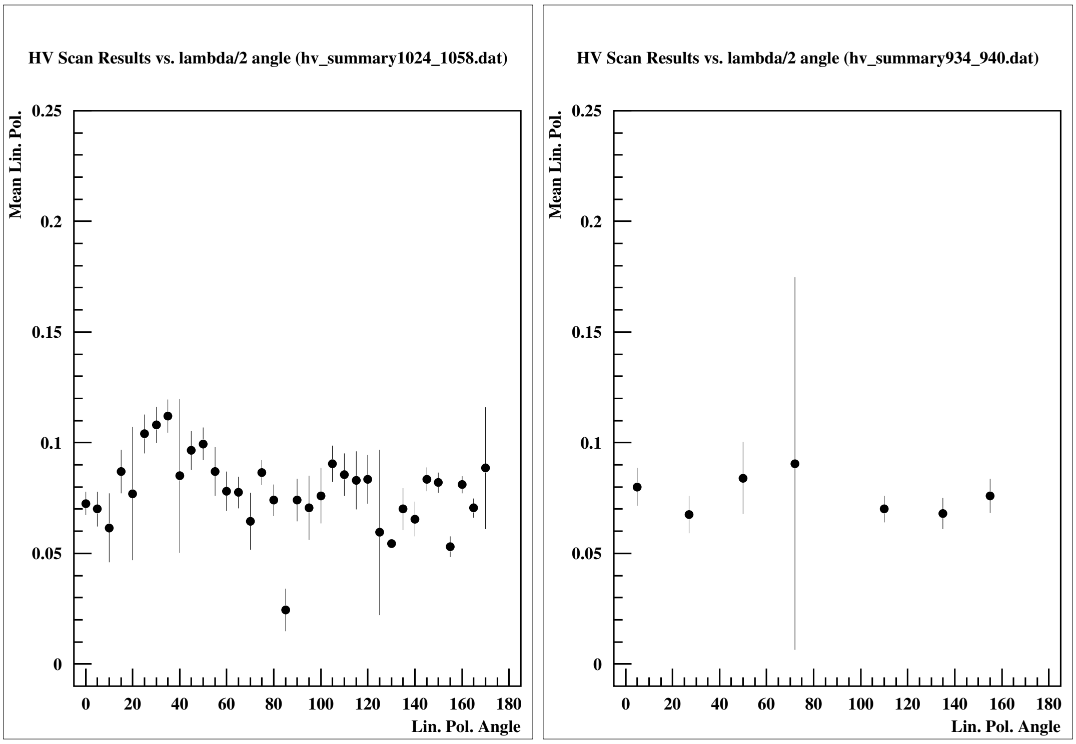

(a) Mean pol. in laser hut (see fig. 6b)

(b) Mean pol. at IP (see fig. 7b)

Figure 5: The mean linear polarization ΔS_1

The mean polarization turns out to be more or less constant:

$$\Delta S_1 = \quad 0.80\% \pm 0.3\% \tag{4}$$
$$\Delta S_3 = 99.67\% \pm 0.2\% \tag{5}$$

If we now compare the voltage settings at a fixed phase angle, we see that the set voltages in the laser hut (fig. 6) differ in the worst case about ± 50 Volts from the optimal voltages at the interaction point (fig. 8). By a look at figure 1 one can see, that a variation of 100 Volts at the maximum of the parabola induces a change in the linear component of $\sim 6\%$. If we assume 99.67% circulary polarized light in the laser hut, then the maximal error on the polarization at the IP is

$$\Delta P_C \simeq \pm 0.5\% \tag{6}$$

The different phase shifts of the components are summarized in table 1:

component/effect	phase (lin. pol. angle)
Hera exit window	$\simeq +\ 2°$
Hera entrance window	$\simeq +10°$
Laser system entrance window	$\simeq +10°$
Mirrors M5/6	$\simeq +15°$
all components(not ventilated)	$\simeq +40°$
laser pipe ventilated	$\simeq +10°$

Table 1: phase shifts of the optical components

2 Conclusion

The polarization studies at the longitudinal polarimeter have shown that we know our circular light polarization at the IP during the 1997 data taking with an accuracy of $\pm 1\%$. This most conservative estimate could be improved if we assumed that the phase of the optical system staid constant over the entire data taking. Unfortunately our optical setup including the additional half-wave plate influences the measured polarization and phase, so that we cannot extract the exact phase out of the data. By comparing the polarization scans at different points in the laser transport system one can extract the effects of the different components.

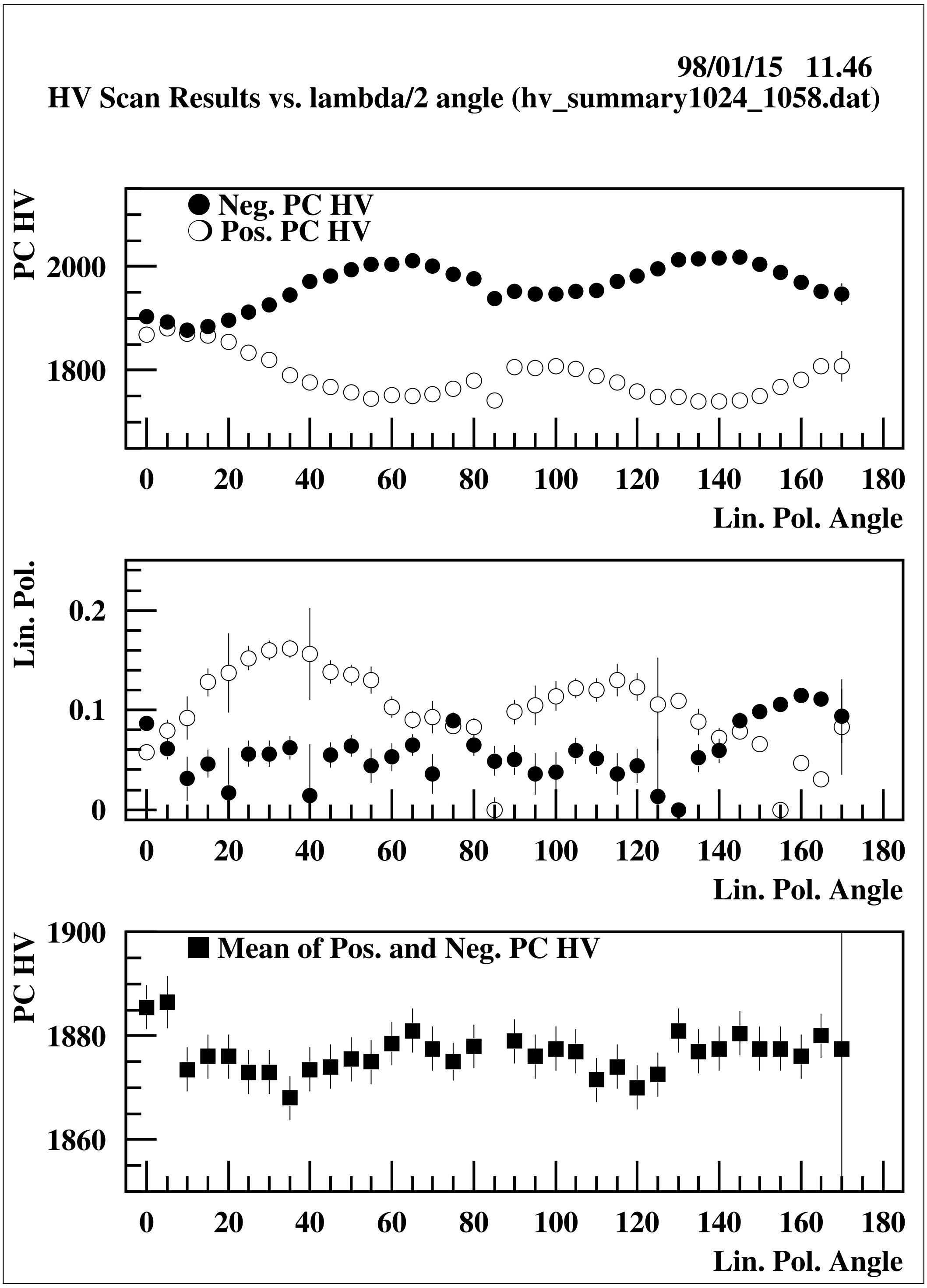

Figure 6: Results of the scan in AB#1, installed in laser hut

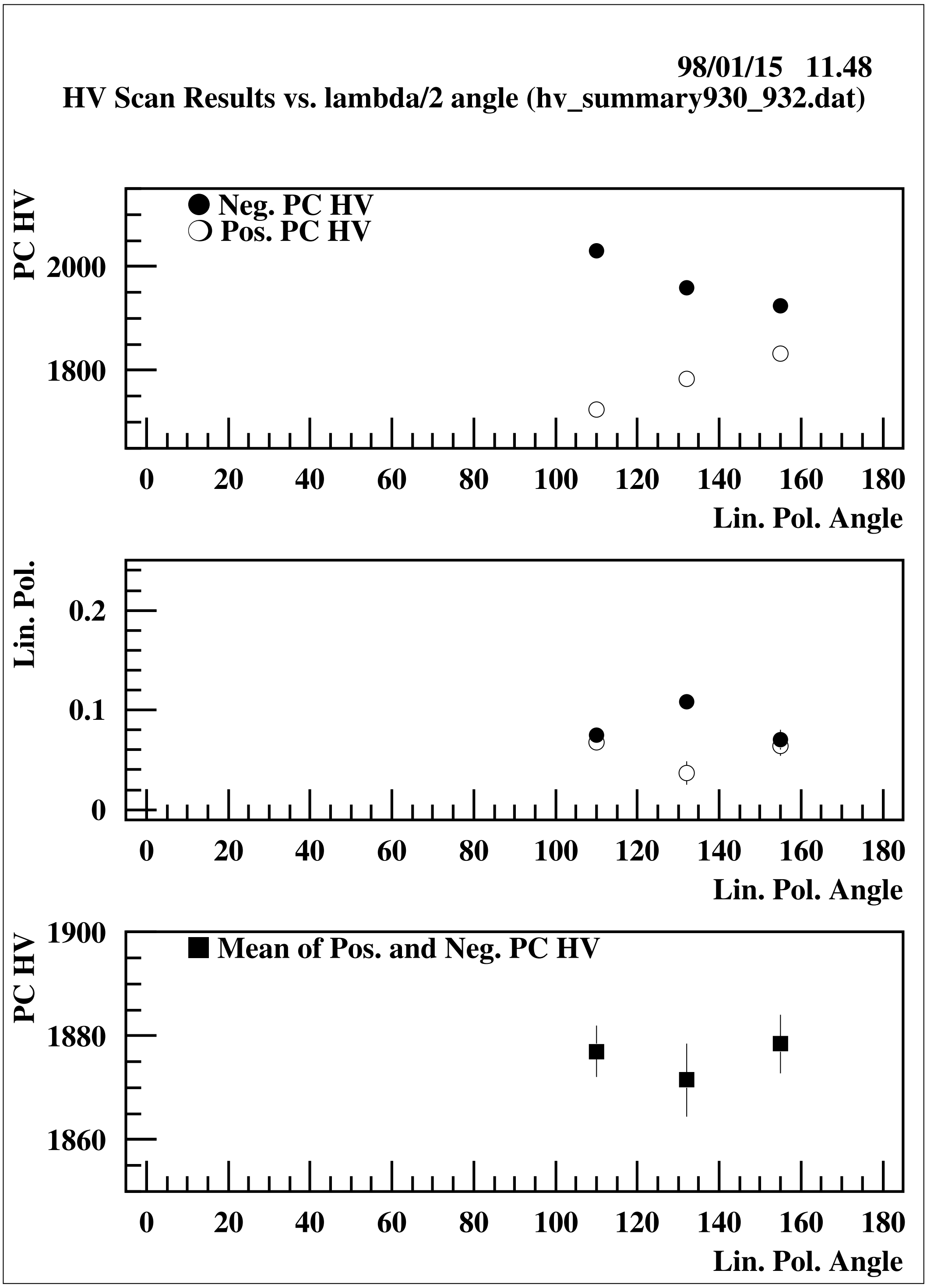

Figure 7: Results of the scan in AB#1, behind Hera exit window, all windows installed

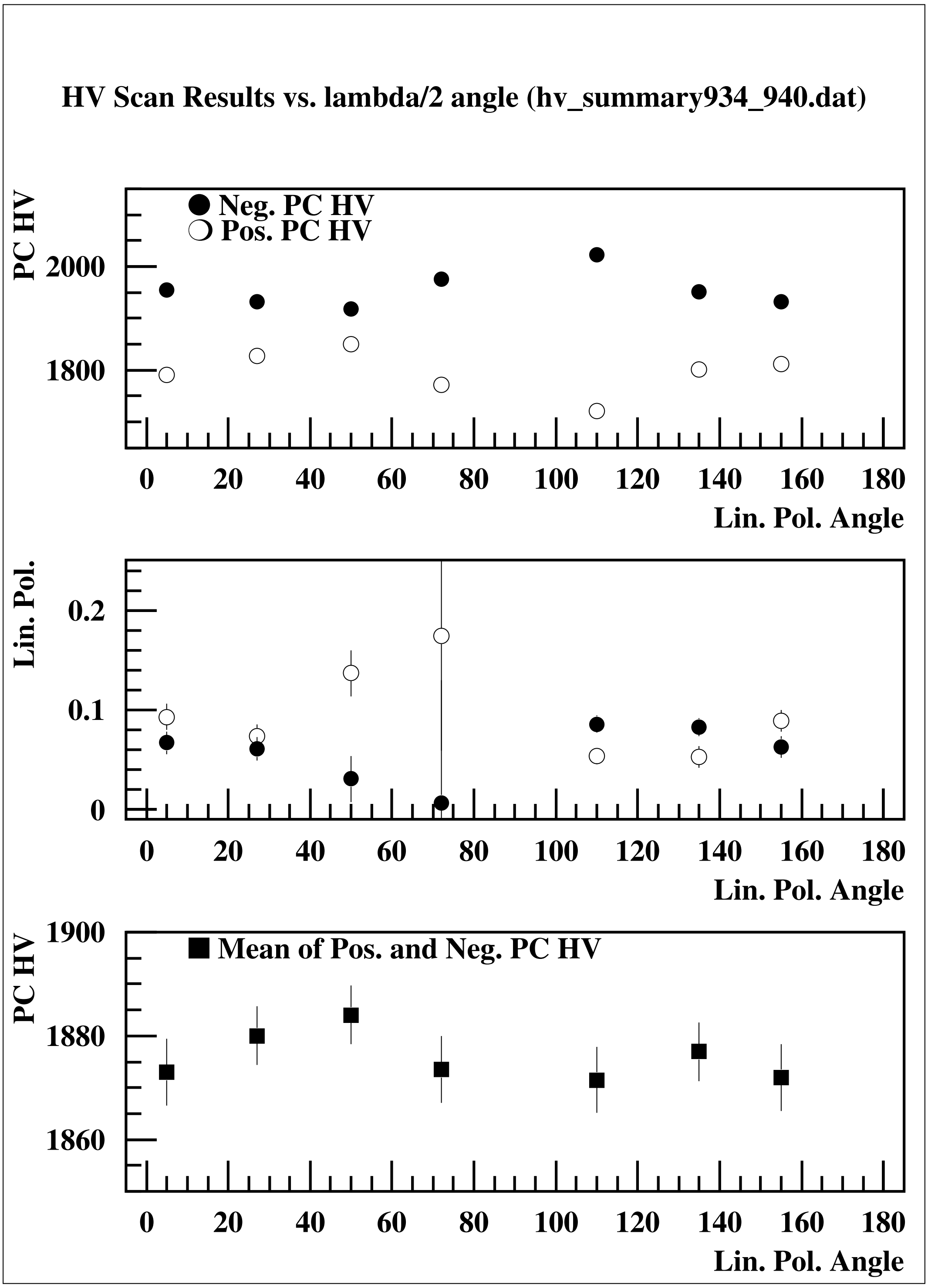

Figure 8: As fig. 7, Hera exit window removed

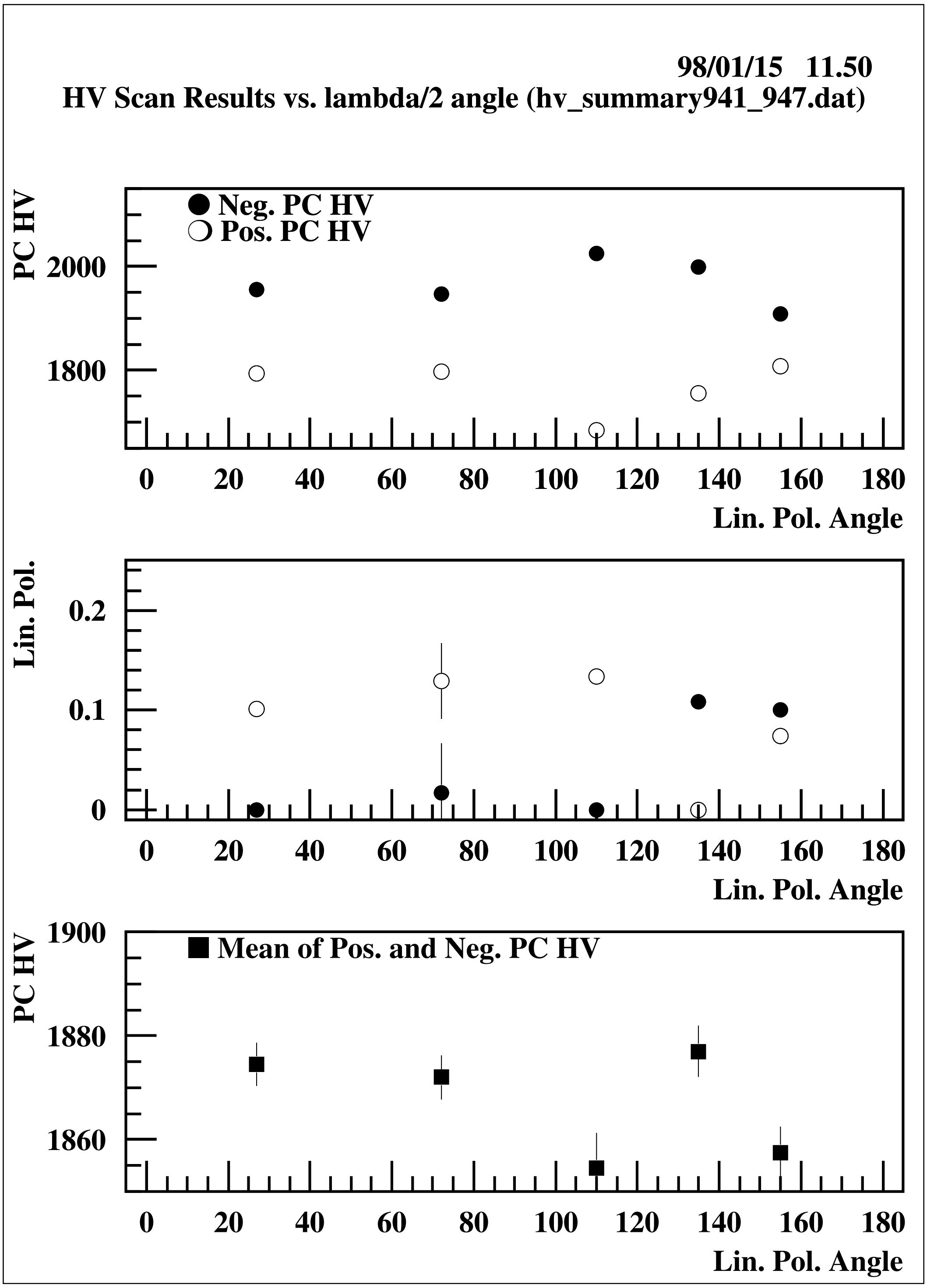

Figure 9: As fig. 8, laser beam pipe ventilated

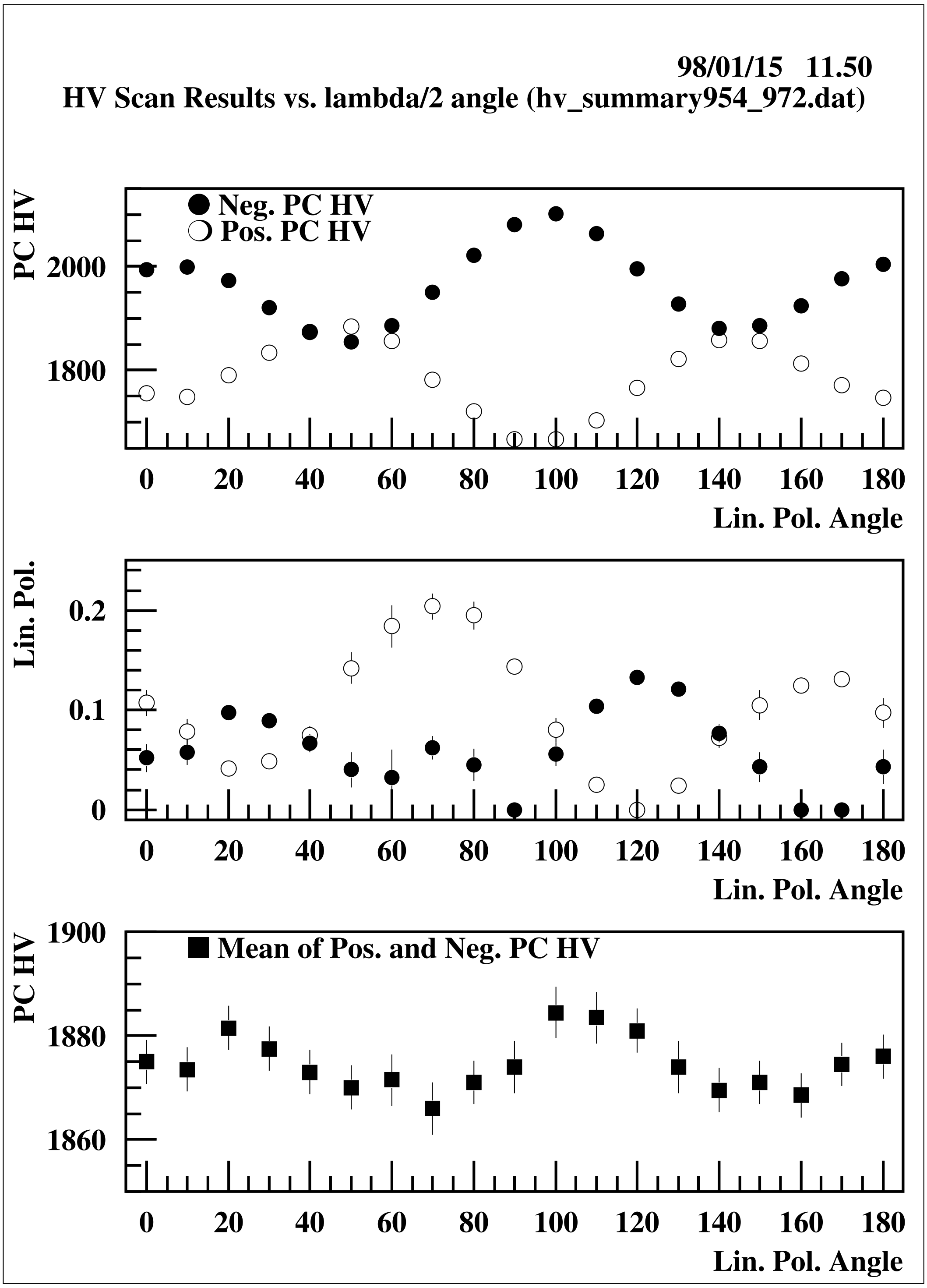

Figure 10: As fig. 9, beam pipe entrance window removed

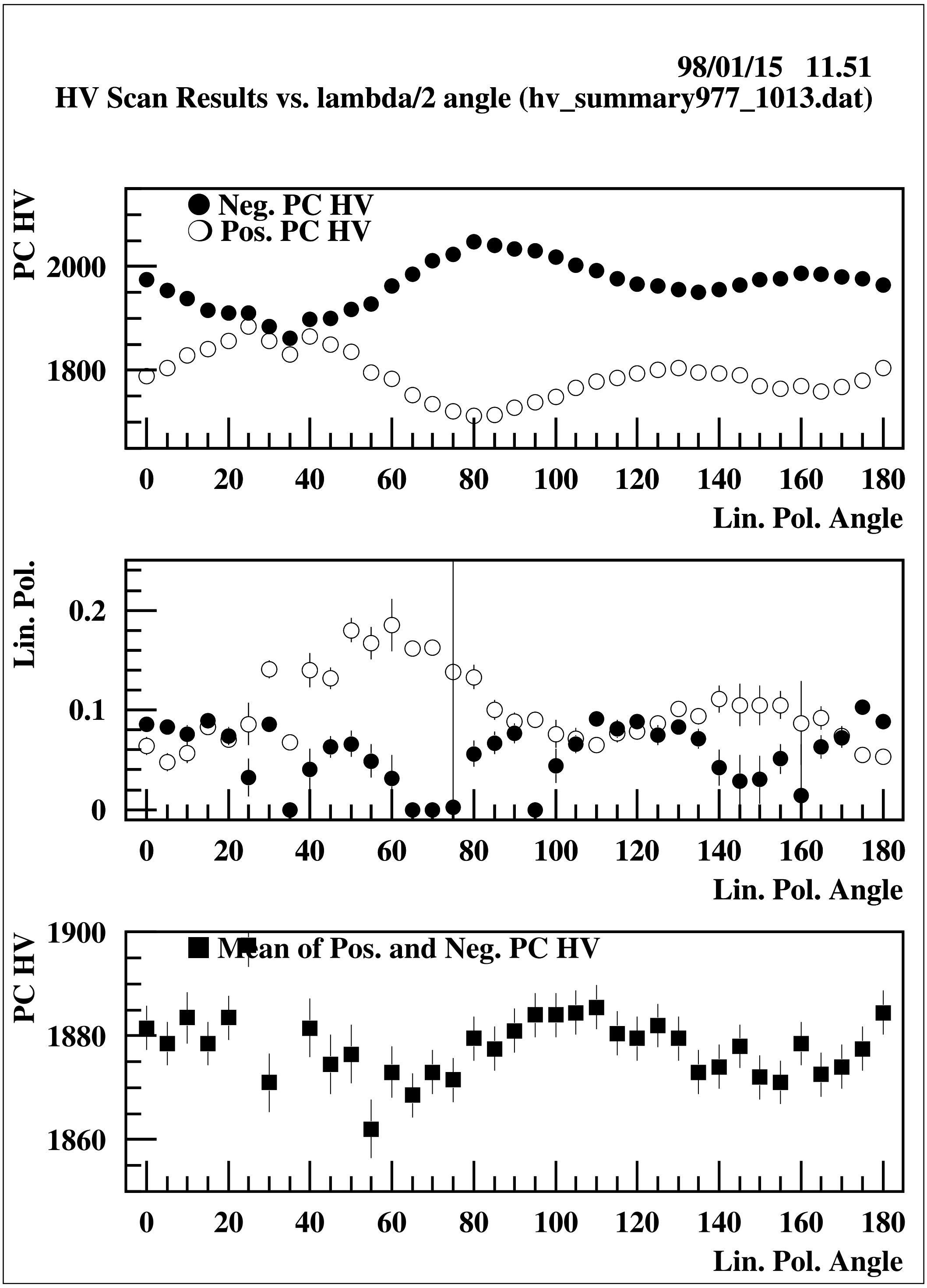

Figure 11: As fig. 10, Hera entrance window removed

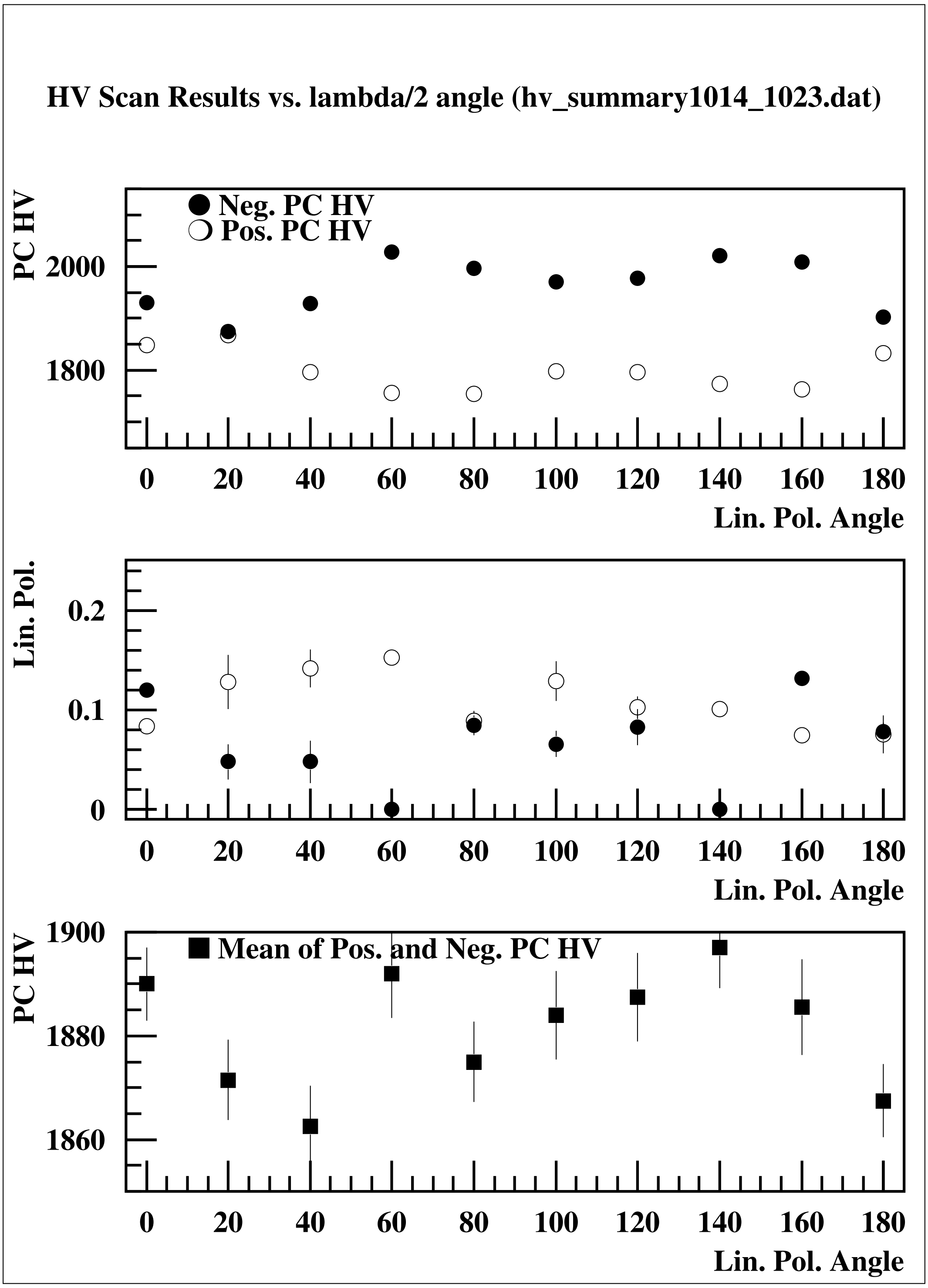

Figure 12: Results of the scan in AB#1, behind M5/6, laser system entrance window removed